Title
Different Single-Enzyme Conformational Dynamics upon Binding Hydrolyzable or Nonhydrolyzable Ligands

Journal
The Journal of Physical Chemistry B, 125(22)

ISSN
1520-6106

Authors
Woo, Sung Oh
Oh, Myungkeun
Alhalhooly, Lina
et al.

Publication Date
2021-06-10

DOI
10.1021/acs.jpcb.1c01589

Peer reviewed

HHS Public Access

Author manuscript

J Phys Chem B. Author manuscript; available in PMC 2022 June 10.

Published in final edited form as:

J Phys Chem B. 2021 June 10; 125(22): 5750–5756. doi:10.1021/acs.jpcb.1c01589.

Different Single-Enzyme Conformational Dynamics upon Binding Hydrolyzable or Nonhydrolyzable Ligands

Sung Oh Woo[1], **Myungkeun Oh**[2], **Lina Alhalhooly**[1], **Jasmin Farmakes**[3], **Arith J. Rajapakse**[4], **Zhongyu Yang**[3], **Philip G. Collins**[4], **Yongki Choi**[1,2,*]

[1]Department of Physics, North Dakota State University, Fargo, North Dakota 58108, United States

[2]Materials and Nanotechnology Program, North Dakota State University, Fargo, North Dakota 58108, United States

[3]Department of Chemistry and Biochemistry, North Dakota State University, Fargo, North Dakota 58108, United States

[4]Department of Physics and Astronomy, University of California, Irvine, California 92697, United States

Abstract

Single molecule measurements of protein dynamics help unveil the complex conformational changes and transitions that occur during ligand binding and catalytic processes. Using high-resolution single molecule nanocircuit techniques, we have investigated differences in the conformational dynamics and transitions of lysozyme interacting with three ligands: peptidoglycan substrate, substrate-based chitin analog, and indole derivative inhibitors. While processing peptidoglycan, lysozyme followed one of two mechanistic pathways for the hydrolysis of the glycosidic bonds: a concerted mechanism inducing direct conformational changes from open to fully closed conformations, or a nonconcerted mechanism involving transient pauses in intermediate conformations between the open and closed conformations. In the presence of either chitin or indole inhibitor, lysozyme was unable to access the fully closed conformation where catalysis occurs. Instead, lysozymes' conformational closures terminated at slightly closed, "excited" conformations that were approximately one quarter of the full hinge-bending range. With the indole inhibitor, lysozyme reached this excited conformation in a single step without any evidence of rate-liming intermediates, but the same conformational motions with chitin involved three hidden, intermediate processes and features similar to the nonconcerted peptidoglycan mechanism. The similarities suggest that these hidden processes involve attempts to accommodate imperfectly aligned polysaccharides in the active site. The results provide a detailed glimpse of the enzyme-ligand interplay at the crux of molecular recognition, enzyme specificity, and catalysis.

[*]**Corresponding Author :** yongki.choi@ndsu.edu.

Author Contributions

The manuscript was written through contributions of all authors. All authors have given approval to the final version of the manuscript.

Supporting Information. Additional materials and methods, Timing of lysozyme activity with peptidoglycan substrate (Table S1), chitin, and IPA (Table S2), Example signals for individual pause events during the fast, nonproductive motions (Figure S1).

The authors declare no competing financial interest.

INTRODUCTION

A central question in biochemistry is the mechanisms that control conformational changes during dynamic protein-ligand interactions. Theoretically, two models have been proposed: proteins have a small number of pre-selected global conformational states to complement ligand structure, or particular ligands induce the protein conformation to adopt their structure.[1–3] Both models are grounded in proteins' remarkable flexibility upon ligand binding, which originates from soft fluctuations of atoms and residues.[4–7] In addition, the catalytic power of enzymes depends on conformational fluctuation and transition, which contribute to their dramatic specificity and the affinity of ligand interactions. Identifying the dynamic properties of protein conformations and protein-ligand interactions improves our understanding of the underlying mechanisms and many biological processes associated with disease development.[8]

Recent advances of single-molecule techniques significantly extend our knowledge of enzyme-ligand interactions by revealing the dynamics of enzyme activity. In studies of T4 lysozyme, single-molecule Forster resonance energy transfer experiments observed dynamic hinge-bending and conformational changes of lysozyme during the hydrolysis of peptidoglycan substrate;[9, 10] and single-molecule nanocircuit techniques have uncovered long-lived intermediate conformations during lysozyme's opening and closing transitions.[11] Recently, a hybrid fluorescence spectroscopic toolkit approach combining several single and ensemble biochemical assays also observed transient conformational states in lysozyme's hinge bending motion, finding these intermediates to be abundant and critical in enzyme catalysis.[12]

In this work, we extend the study of lysozyme's conformational dynamics by comparing intermediary transients formed between lysozyme and three different substrates. Taking advantage of the lysozyme nanocircuit approach and its temporal resolution of 2 μs, we compared lysozyme interacting with peptidoglycan substrate, substrate-based chitin analog, and nonspecific indole-3-propinoic acid (IPA) inhibitor. Long- and short-lived pauses were observed for each type of enzyme-ligand interaction, revealing short-lived conformational states that might be intermediates, alternate transition pathways, or conformational dead ends. The nanocircuit technique enabled the collection of single-molecule data from three different substrates, the quantitative analysis of which produced detailed transitional kinetics and free energy profiles revealing how lysozyme interacts differently with each ligand.

METHODS

A pseudo wild-type T4 lysozyme mutant (C54T/C97A/S90C) was synthesized via site-directed mutagenesis and expressed from *Escherichia coli* cells, as previously described.[13–15] The single-walled carbon nanotube field effect transistor (SWNT FET) fabricated by CVD synthesis and standard lithography techniques[16] was soaked in a solution of bifunctional linker molecule, *N*-(1pyrenyl)maleimide in ethanol (1mM) for 30 min, washed with 0.1% Tween-20 in ethanol and deionized water, and then incubated in the lysozyme solution (5.4 μM in PBS) for 60 min. On average, about 1 protein attachment in every two devices was confirmed by imaging the devices with atomic force microscopy

(Figure 1a). Once the attachment conditions were determined for a given batch of enzyme, the attachment yield remained constant. The scheme has been used successfully to produce specific, single-protein attachments across many (>100) devices and multiple lysozyme variants.[11, 16–18] Afterward, the device was rinsed with wash buffer (5 mM KCl, 10 mM Na_2HPO_4, 0.05% Tween-20, pH 7) and inserted into a home-built microfluidic flow cell to perform high-bandwidth electrical measurements. The devices were monitored (> 10 min) in PBS solutions or substrates (peptidoglycan, chitin, indole-3-propinoic acid) suspended in PBS (25 μg/ml). The source-drain current $I(t)$ was measured using a FEMTO DLPCA-200 low noise preamplifier operating at 10^8 V/A gain (1.8 μs rise time) with source-drain bias of 100 mV and electrolyte potential held constant at a bias of −0.1 to −0.4 V (vs. Pt pseudo-reference electrode). Similar methods have been described in previous publications.[11, 16–18] Materials and methods are described in more detail in the Supporting Information.

RESULTS AND DISCUSSION

As in previous work with single-lysozyme nanocircuits, electronic recordings clearly resolved the conformational dynamics-driven interactions with peptidoglycan substrate (Figure 1). Measured in buffer without peptidoglycan, the nanocircuit's source-drain current fluctuations $\Delta I(t)$ showed featureless current noise with a simple Gaussian distribution (Figure 1b). Peptidoglycan in the solution generated additional two-level $\Delta I(t)$ fluctuations (Figure 1c). Following the determinations of previous studies,[16] the $\Delta I(t) = 0$ baseline was associated with the lowest-energy, open conformation, in which lysozyme sits when substrate is absent; and then $\Delta I(t)$ increased as lysozyme's two main subdomains closed upon the substrate in an 8 Å, hinge-bending motion.[19–21] The two distinct signal levels shown in Figure 1c represent measurements of lysozyme's open and closed conformations and the dynamics of motions between these two states. Each individual closure can be characterized by a waiting time in the open state (τ_{open}), a duration in the closed state (τ_{closed}) and an instantaneous fluctuation rate $k = 1/(\tau_{open} + \tau_{closed})$. With peptidoglycan, previous single-molecule nanocircuit and fluorescence resonance energy transfer experiments revealed that the closures readily separated into two distinct categories: the enzyme spends multiple seconds processing at a slow, enzymatic turnover rate of 20 – 90 Hz, and then it transitions to a fast, nonproductive movement at 200 – 400 Hz.[16, 19] The two categories of motion do not intermix, so the enzyme's instantaneous state can be determined by inspecting only a few events. In Figure 1c, for example, relatively fast repetitions at $k = 326\ s^{-1}$ illustrate the latter category of catalytically nonproductive motions associated with encountering peptidoglycan's nonhydrolyzable cross-links.[9, 14, 22] Figure 1d shows the category corresponding to catalytic hydrolysis of the peptidoglycan, characterized by slower rates $k = 52\ s^{-1}$ and durations $<\tau_{closed}> = 3.7$ ms that lasted almost 30 times longer than the nonproductive closures. For both the nonproductive and catalytic distributions, the magnitude of current fluctuations can be converted into an effective gating voltage $\Delta V_{eff} = \Delta I(dI/dV)^{-1}$ that is a device-independent measure of the extent of conformational motion; the value $\Delta V_{eff} = 180$ mV observed here matches previous lysozyme nanocircuit work[16, 18] and confirms our assignments to the open and closed conformations.

With both peptidoglycan and nonhydrolyazable substrates, lysozyme exhibited transient pauses at conformations intermediate between the open and closed states, and these

intermediates were the main focus of this study. The segment of $\Delta I(t)$ signal in Figure 1d is an illustrative example selected for its unusually dense collection of pauses with peptidoglycan. This one example shows transient pauses occuring during an open-to-closed transition (at $t = 7$ ms), a closed-to-open transition ($t = 10$ ms), and an open-to-open fluctuation ($t = 52$ ms). These three types of pauses, along with a closed-to-closed transient, form a two-by-two matrix of transition probabilities, kinetics, and complexity that extend the simple, open-or-closed lysozyme model. All four types contribute to a single, small-amplitude peak in the $\Delta I(t)$ histogram at $\Delta V_{eff} = 94$ mV (Figure 1c,d), corresponding to an intermediate conformation that is approximately halfway closed.

For detailed quantitative and statistical analysis of each type of transient pause, more than 600 seconds of single-molecule $I(t)$ recordings were collected with each substrate. Pauses were then identified with threshold filters, categorized, and accumulated into probability density (PD) functions. Each PD was fitted to the N-consecutive Poisson distribution,

$$\mathrm{P}(t, \lambda, N) = \frac{\lambda^N t^{N-1}}{\Gamma(N)} e^{-\lambda t}, \quad (1)$$

where λ is the shared rate, N is the number of Poisson processes degenerated in the durations, t is pause duration, and Γ is the gamma function.[23] The results obtained with peptidoglycan are depicted graphically in Figure 2 and in tabular form with detailed kinetic parameters in the Supporting Information (Table S1). The results obtained with chitin and IPA are presented in Figure 3 and Table S2.

Focusing first on peptidoglycan, we observe that lysozyme's slow, catalytic motions were characterized by multiple transition pathways (Figure 2a,b). Approximately 75% of opening and closing movements proceeded in a single step without interruption. The simplest pathway for enzyme catalysis is frequently represented by the Michaelis-Menten mechanism $E + S \rightleftharpoons ES_1 \rightharpoonup EP_1 \rightharpoonup E + P$, in which an enzyme E and a substrate S bind to form an ES_1 complex, transform into an EP_1 complex, and then separate, releasing the product P.[24] While this simple representation was appropriate for the majority of transitions, the remaining 25% transitions were interrupted by transient pauses. The PDs of pauses during opening and pauses during closing are overlaid in Figure 2a to highlight the near-identical kinetics in both directions. Both PDs peaked at durations of 450 to 500 μs and fit Eq. 1 with $N = 4$, indicating at least four processes and three intermediate states.

Figure 2b is a schematic energy landscape depicting the direct and indirect pathways and the exact probabilities for each. Black arrows represent single-step transitions in each catalytic half-cycle, and red or blue arrows suggest the indirect pathways through additional intermediates. When closing upon peptidoglycan, 73% of events proceeded directly to the EP state in a single step and 27% were interrupted by a transient pause at an intermediate configuration. From this intermediate, 19% of the motions reversed themselves back to the open conformation (green), with only 8% of the motions progressing into the completely closed EP state (red). Similar probabilities were observed for the second half of the catalytic cycle: 77% of transitions opened in a single step, 9% of transitions proceeded through an

intermediate state to reopen (blue), and 14% of transitions reclosed after pausing in an intermediate state (green).

Statistical analysis found the opening and closing pauses to be uncorrelated and largely governed by the same probability $p \approx 75\%$ as the primary direct transitions. In other words, the fraction of complete cycles interrupted by 0, 1, or 2 pauses was approximately equal to $(1\text{-}p)^2$, $2p(1\text{-}p)$, and p^2, as one would predict for a memoryless system in which opening and closing were independent processes. Figure 1d has been constructed to provide an illustrative but rare example of a cycle with 2 visible pauses (before and after $t = 10$ ms), a coincidence observed in only 1% of all events.

Analysis of the transition pathways during lysozyme's nonproductive opening and closing revealed two major differences from the catalytic motions described above. Firstly, the PD for transient pauses fit Eq. 1 with $N = 1$, indicating a single intermediate state (Figure 2c) that did not include multiple processes. The mean duration for pauses in this intermediate was 380 to 410 μs, comparable to the most probable durations (i.e. the peak of the PD) in Figure 2a. Secondly, almost all nonproductive transients occurred during aborted closing motions, examples of which are shown in Figure S1. 30% of all closing motions exhibited interruptions, with 29% of the events returning to the fully open configuration from the intermediate state. Only 1% of all events paused in the intermediate before proceeding to the closed configuration, and only 2% of all reopening motions exhibited any transient pauses at all (Figure 2).

The peptidoglycan results described here are consistent with a mechanistic model proposed in previous work.[11] Specifically, the majority of lysozyme motions occur along a simple, short pathway in which lysozyme smoothly and continuously changes its conformation between open and closed without accessing intermediate conformations. Lysozyme's closure twists the *N*-acetylmuramic acid (NAM) in peptidoglycan from an undistorted chair to a distorted skew boat conformation, straining the glycosidic bond to the adjacent *N*-actylglucosamine (NAG) residue and making it susceptible to hydrolysis.[25] This catalytic pathway is inaccessible when the NAG-NAM subunit is misaligned with lysozyme's active site, so we previously proposed[11] that a nonconcerted pathway of intermediate conformations might provide an opportunity for the peptidoglycan side chains to reposition. Figure 2 provides evidence for intermediate conformations in which lysozyme pauses while partly closed, perhaps allowing for limited realignment and stabilization of the lysozyme-peptidoglycan complex. The experimental ratio of 8% successes to 19% reversals suggests that this realignment enables the fully closed conformation in about 1/3 of the attempts, realizing a modest improvement in the closure probability. On the other hand, sometimes lysozyme closes upon an nonhydrolyzable cross-link. In these nonproductive motions, the intermediates are either inaccessible or not meaningful, leading to the near-complete reversal of partial closures in a single step ($N = 1$), as shown in Figures 2c and 2d. Regardless of the correct interpretation, we note that all of the intermediates are associated with partly-closed conformations and therefore not directly involved in the chemical step of glycosidic hydrolysis.[10, 11]

The near symmetry of transient kinetics during closing and opening suggests that the intermediate states play equally important roles in both parts of the catalytic cycle. The lack of correlated pairings, on the other hand, makes it seem unlikely that the reopening pauses are caused by certain peptidoglycan misorientations or symmetric, constrained conformational pathways. Instead, intermediate states might help the fraction of saccharide diffuse out of the active site, a product release step that is not energetically favorable. There might also be error-checking roles that halt reopening after unsuccessful hydrolysis. Experimentally, lysozyme returned to its closed conformation in 14% of partial re-openings when it was closed upon hydrolyzable polysaccharides (Figure 2b), whereas the same states only reverted 0.4% of openings upon the nonhydrolyzable cross-links. The difference, along with the different failure rates for closing upon cross-links, indicates that the essential structural feature of ligands plays a dominant role in lysozyme's conformational dynamics.

To further examine this idea of ligand dependence, we applied a similar analysis of intermediate states to the conformational dynamics of lysozyme with two additional substrates, a chitin analog of peptidoglycan and a non-specific IPA inhibitor. Chitin is a homopolysaccharide, structurally similar to peptidoglycan with no tetra peptide side chain in *N*-acetylmuramic acid residue.[26] Lysozyme binds to chitin because of structural similarity with peptidoglycan, but it cannot hydrolyze chitin.[27, 28] On the other hand, indole derivatives including IPA have been found to be substrate-competing inhibitors that nonspecifically bind to lysozyme's active site and inhibit activity.[29, 30] These charactistics made IPA and chitin good candidates for investigating the effects of ligand structures on lysozyme's conformational motions.

Figure 3 shows that dynamic $\Delta I(t)$ fluctuations continued to be observed when the lysozyme nanodevice was probed with either IPA or chitin. These fluctuations, along with $\Delta I(t)$ histograms fitting two or three Gaussian peaks, indicated activity beyond lysozyme's thermal motions (Figure 1b) and supported the premise that lysozyme actively interacted with both ligands. On the other hand, smaller fluctuation magnitudes and ΔV_{eff} values indicated that lysozyme was no longer achieving the same degree of closure with these ligands. With IPA, for example, lysozyme's transient state was located at $\Delta V_{eff} = 42 \pm 3$ mV (Figure 3a), a value less than half of the intermediate state described above for peptidoglycan and only 23% of the value of the fully-closed conformation. The direct relationship between ΔV_{eff} and mechanical hinge-bending indicates that these transient conformations were only slight motions away from the open conformation.

Additional analysis of the kinetics of lysozyme-IPA interactions further suggested very weak binding. The transition rate between them was measured to be 750 s^{-1}, more than twice the rate for the fast, nonproductive closings and openings upon peptidoglycan cross-links. The transients lasted only 0.12 ms, on average, and the PD fit to Eq. 1 with $N = 1$. These detailed parameters, which are summarized in Table S2 and depicted in Figure 3c, indicated a single-step process into and out of a slightly-closed conformational shoulder of the open conformation's potential well, as illustrated in the inset of Figure 3c. The IPA interaction could be described as inducing a briefly-occupied, 'excited' conformation in lysozyme, with no evidence of rate-limiting intermediates.

These observations are consistent with IPA's chemical structure. Since IPA does not have polysaccharide units nor tetra peptides, it cannot induce lysozyme's fully closed conformation or access any of the intermediates ES_i for aligning ligands in the active site. According to theoretical modeling, nonspecific interactions cause minimal conformational changes in lysozyme.[31] Instead, IPA enters a hydrophobic region of the active site and may cause distortion of the active site, along with charge redistribution of lysozyme.[29, 30]

Similar results were observed for nonspecific lysozyme-chitin interactions. When chitin was present, transient fluctuations occurred to two excited conformations (named ***1*** and ***2***) located at $\Delta V_{eff} = 25 \pm 2$ mV and 40 ± 2 mV, again small fractions of lysozyme's full range. As with IPA, fluctuations occurred rapidly at rates of 500 to 550 s^{-1} and with short average durations of 0.16 and 0.09 ms, all indicative of weak interactions. However, the duration PDs with chitin indicated $N = 3$ (for ***1***) and $N = 2$ (for ***2***) transition processes containing additional hidden intermediates. The difference between $N = 1$ for IPA and $N > 1$ for chitin suggests two very different interactions, and we conclude that the similar ΔV_{eff} values were coincidental rather than evidence that both molecules induce the same conformation in lysozyme.

The presence of two distinct intermediate states ***1*** and ***2*** with chitin enabled further comparison and analysis of higher order transitions and kinetics. For example, the probability was nearly identical for transitions into either ***1*** or ***2***, with neither state being favored. This randomization probably indicates that both excited conformations were well within lysozyme's range of thermal fluctuations. On the other hand, the average duration spent in ***1*** was nearly twice as long as for ***2***, so Figure 3d depicts ***1*** at a lower, more thermodynamically favorable energy. When leaving state ***1*** or ***2***, thermalization again randomized the process, so that the probability of lysozyme returning to the ground state was only $71 \pm 3\%$. This thermalization, which likely involved the $N = 2$ intermediating steps, led to a memoryless series of high-order transitions like ***0-1-2-0***, ***0-1-2-1-0***, etc. with probabilities $p(n) = 0.71^n$ for each order n. Exact values from one data set are provided in Tables 1 and S2, demonstrating that random transitions between ***1*** and ***2*** persisted at all orders.

These chitin transition probabilities reveal the third instance where one of two mechanistic pathways is favored by a 70% probability bias, despite evidence of memoryless thermalization. To recapitulate, lysozyme closes in a single step upon peptidoglycan with a 70% probability, pausing at an intermediate in the other 30% of cases. From that intermediate state, lysozyme reopens with a 70% probability but fully closes in the other 30% of attempts (except with nonhydrolyzable crosslinks, which always reopen). And when partly closed on chitin, lysozyme again has a 70% probability of reopening, with the other 30% of events resulting in a transition between excited states ***1*** and ***2***. All three cases maintain a similar bias equivalent to $\Delta G = 0.5$ to 0.6 kcal/mol, and we conclude that the energy landscape for different conformations is indeed biased towards certain pathways and configurations. However, the magnitude of the energy difference is essentially equal to thermal energy at room temperature and only a fraction of the energy of a strained bond or a weak hydrogen bond. Consequently, this bias might be undetectable in structural models

or high-temperature molecular dynamics simulations. Perhaps thermal fluctuations play an unexplored role in achieving the bias for one transition pathway over another.

Another important comparison can be drawn between the number of intermediate processes observed with peptidoglycan, IPA, and chitin. In the two noncatalytic cases of IPA and nonhydrolyazable peptidoglycan crosslinks, lysozyme exited its transient conformation in a single step $N = 1$ with no evidence of intermediate processes. Transient conformations testing chitin and peptidoglycan, on the other hand, involved multiple processes $N =$ 2 to 4. Above, we have proposed that peptidoglycan's $N = 4$ processes may involve critical reorientations of peptidoglycan's NAG-NAM subunit that stabilize the lysozyme-peptidoglycan complex for catalysis.[21, 32] Similar orientational realignments are possible for the acetamido group in chitin's NAG residues,[28] but incomplete adoption and alignment of this peptide-free homopolysaccharide probably limits the full range of lysozyme's hinge motion. Our observation of conformational transitions between open and excited conformations agrees with previous lysozyme studies with chitin,[27, 28] and clearly demonstrates the allosteric role of the peptide in peptidoglycan and its contribution to the enzyme specificity and overall catalytic activity. Taken together, results from chitin and IPA reveal that the rejection of those ligands takes place in excited conformations that are far from the closed conformation, and that chitin and peptidoglycan share similar hidden processes in partly-closed conformations. These transient, intermediary conformations clearly depend on the ligand structures and play crucial roles in the overall process called molecular recognition.

CONCLUSIONS

Using the high-resolution single lysozyme nanocircuit approach, we have observed ligand-dependent, distinct conformational states of lysozyme and dynamic interconversion between open, intermediate, and fully closed conformations. When interacting with the peptidoglycan substrate, lysozyme was able to smoothly reach the fully closed, hydrolysis-ready conformation with approximately 10% of interrupting pauses because of the nonconcerted mechanism. In contrast, the dynamic interactions with peptide-free chitin and nonspecific inhibitor IPA showed minimal conformational changes of lysozyme from open to very slightly closed, excited conformations with fast transition rates. Despite having similarities, the presence of hidden intermediates and two excited conformations in the chitin interactions helped make lysozyme's binding and unbinding kinetics with chitin very distinct from those with either IPA or peptidoglycan. These observations of ligand-dependent conformational dynamics reveal the trajectories of the induced-fit mechanism for enzyme catalysis, in which ligand structure couples to conformational changes on microsecond time scales to achieve enzyme specificity and catalysis.

Supplementary Material

Refer to Web version on PubMed Central for supplementary material.

ACKNOWLEDGMENT

This research was supported financially by the NIH/NIGMS under Award Number R15GM122063 and P20GM109024.

REFERENCES

(1). Vogt AD; Di Cera E, Conformational Selection or Induced Fit? A Critical Appraisal of the Kinetic Mechanism. Biochemistry 2012, 51, 5894–5902. [PubMed: 22775458]

(2). Johnson KA, Role of induced fit in enzyme specificity: a molecular forward/reverse switch. J. Biol. Chem 2008, 283, 26297–301. [PubMed: 18544537]

(3). Sullivan SM; Holyoak T, Enzymes with lid-gated active sites must operate by an induced fit mechanism instead of conformational selection. Proc Natl Acad Sci U S A 2008, 105, 13829–34. [PubMed: 18772387]

(4). Bakan A; Bahar I, The intrinsic dynamics of enzymes plays a dominant role in determining the structural changes induced upon inhibitor binding. Proc. Natl. Acad. Sci. U. S. A 2009, 106, 14349–14354. [PubMed: 19706521]

(5). Bahar I; Lezon TR; Yang LW; Eyal E, Global Dynamics of Proteins: Bridging Between Structure and Function. In Annual Review of Biophysics, Vol 39, Rees DC; Dill KA; Williamson JR, Eds. Annual Reviews: Palo Alto, 2010; Vol. 39, pp 23–42.

(6). Meireles L; Gur M; Bakan A; Bahar I, Pre-existing soft modes of motion uniquely defined by native contact topology facilitate ligand binding to proteins. Protein Sci. 2011, 20, 1645–1658. [PubMed: 21826755]

(7). Doruker P; Atilgan AR; Bahar I, Dynamics of proteins predicted by molecular dynamics simulations and analytical approaches: Application to alpha-amylase inhibitor. Proteins 2000, 40, 512–524. [PubMed: 10861943]

(8). Tokuriki N; Tawfik DS, Protein Dynamism and Evolvability. Science 2009, 324, 203–207. [PubMed: 19359577]

(9). Lu HP, Single-Molecule Protein Interaction Conformational Dynamics. Curr. Pharm. Biotechno 2009, 10, 522–531.

(10). Lu M; Lu HP, Revealing Multiple Pathways in T4 Lysozyme Substep Conformational Motions by Single-Molecule Enzymology and Modeling. J. Phys. Chem. B 2017, 121, 5017–5024. [PubMed: 28425708]

(11). Akhterov MV; Choi Y; Olsen TJ; Sims PC; Iftikhar M; Gul OT; Corso BL; Weiss GA; Collins PG, Observing Lysozyme's Closing and Opening Motions by High-Resolution Single-Molecule Enzymology. ACS Chem. Bio 2015, 10, 1495–1501. [PubMed: 25763461]

(12). Sanabria H; Rodnin D; Hemmen K; Peulen T-O; Felekyan S; Fleissner MR; Dimura M; Koberling F; Kühnemuth R; Hubbell W; Gohlke H; Seidel CAM, Resolving dynamics and function of transient states in single enzyme molecules. Nat. Commun 2020, 11, 1231. [PubMed: 32144241]

(13). Yang Z; Jiménez-Osés G; López CJ; Bridges MD; Houk KN; Hubbell WL, Long-Range Distance Measurements in Proteins at Physiological Temperatures Using Saturation Recovery EPR Spectroscopy. J. Am. Chem. Soc 2014, 136, 15356–15365. [PubMed: 25290172]

(14). Choi Y; Moody IS; Sims PC; Hunt SR; Corso BL; Seitz DE; Blaszczak LC; Collins PG; Weiss GA, Single-Molecule Dynamics of Lysozyme Processing Distinguishes Linear and Cross-Linked Peptidoglycan Substrates. J. Am. Chem. Soc 2012, 134, 2032–2035. [PubMed: 22239748]

(15). Woo SO; Froberg J; Pan Y; Tani S; Goldsmith BR; Yang Z; Choi Y, Protein Detection Using Quadratic Fit Analysis near the Dirac Point of Graphene Field-Effect Biosensors. ACS Appl. Electron. Mater 2020, 2, 913–919. [PubMed: 32550598]

(16). Choi YK; Moody IS; Sims PC; Hunt SR; Corso BL; Perez I; Weiss GA; Collins PG, Single-Molecule Lysozyme Dynamics Monitored by an Electronic Circuit. Science 2012, 335, 319–324. [PubMed: 22267809]

(17). Choi Y; Moody IS; Sims PC; Hunt SR; Corso BL; Seitz DE; Blaszcazk LC; Collins PG; Weiss GA, Single-Molecule Dynamics of Lysozyme Processing Distinguishes Linear and Cross-Linked Peptidoglycan Substrates. J. Am. Chem. Soc 2012, 134, 2032–2035. [PubMed: 22239748]

(18). Choi Y; Olsen TJ; Sims PC; Moody IS; Corso BL; Dang MN; Weiss GA; Collins PG, Dissecting Single-Molecule Signal Transduction in Carbon Nanotube Circuits with Protein Engineering. Nano Lett. 2013, 13, 625–631. [PubMed: 23323846]

(19). Lu HP, Single-molecule spectroscopy studies of conformational change dynamics in enzymatic reactions. Curr. Pharm. Biotechno 2004, 5, 261–269.

(20). Faber HR; Matthews BW, A mutant T4 lysozyme displays five different crystal conformations. Nature 1990, 348, 263–266. [PubMed: 2234094]

(21). Kuroki R; Weaver L; Matthews B, A covalent enzyme-substrate intermediate with saccharide distortion in a mutant T4 lysozyme. Science 1993, 262, 2030–2033. [PubMed: 8266098]

(22). Chen Y; Hu DH; Vorpagel ER; Lu HP, Probing single-molecule T4 lysozyme conformational dynamics by intramolecular fluorescence energy transfer. J. Phys. Chem. B 2003, 107, 7947–7956.

(23). Floyd DL; Harrison SC; van Oijen AM, Analysis of Kinetic Intermediates in Single-Particle Dwell-Time Distributions. Biophys J 2010, 99, 360–366. [PubMed: 20643053]

(24). Johnson KA; Goody RS, The Original Michaelis Constant: Translation of the 1913 Michaelis-Menten Paper. Biochemistry-Us 2011, 50, 8264–8269.

(25). Choi Y; Weiss GA; Collins PG, Single molecule recordings of lysozyme activity. Phys. Chem. Chem. Phys 2013, 15, 14879–14895. [PubMed: 23752924]

(26). Stryer L, Biochemistry 4th ed.; W. H. Freeman and Company: 1995.

(27). Mirelman D; Kleppe G; Jensen HB, Studies on the Specificity of Action of Bacteriophage T4 Lysozyme. Eur. J. Biochem 1975, 55, 369–373. [PubMed: 1201752]

(28). Kleppe G; Vasstrand E; Jensen HB, The Specificity Requirements of Bacteriophage T4 Lysozyme. Eur. J. Biochem 1981, 119, 589–593. [PubMed: 7308203]

(29). Shinitzky M; Katchalski E; Grisaro V; Sharon N, Inhibition of lysozyme by imidazole and indole derivatives. Arch. Biochem. Biophys 1966, 116, 332–343. [PubMed: 5961840]

(30). Morton A; Matthews BW, Specificity of ligand binding in a buried nonpolar cavity of T4 lysozyme: Linkage of dynamics and structural plasticity. Biochemistry 1995, 34, 8576–8588. [PubMed: 7612599]

(31). Warshel A; Levitt M, Theoretical Studies of Enzymic Reactions - Dielectric, Electrostatic and Steric Stabilization of Carbonium-Ion in Reaction of Lysozyme. J Mol Biol 1976, 103, 227–249. [PubMed: 985660]

(32). Grütter MG; Matthews BW, Amino acid substitutions far from the active site of bacteriophage T4 lysozyme reduce catalytic activity and suggest that the C-terminal Lobe of the enzyme participates in substrate binding. J. Mol. Bio 1982, 154, 525–535. [PubMed: 7077670]

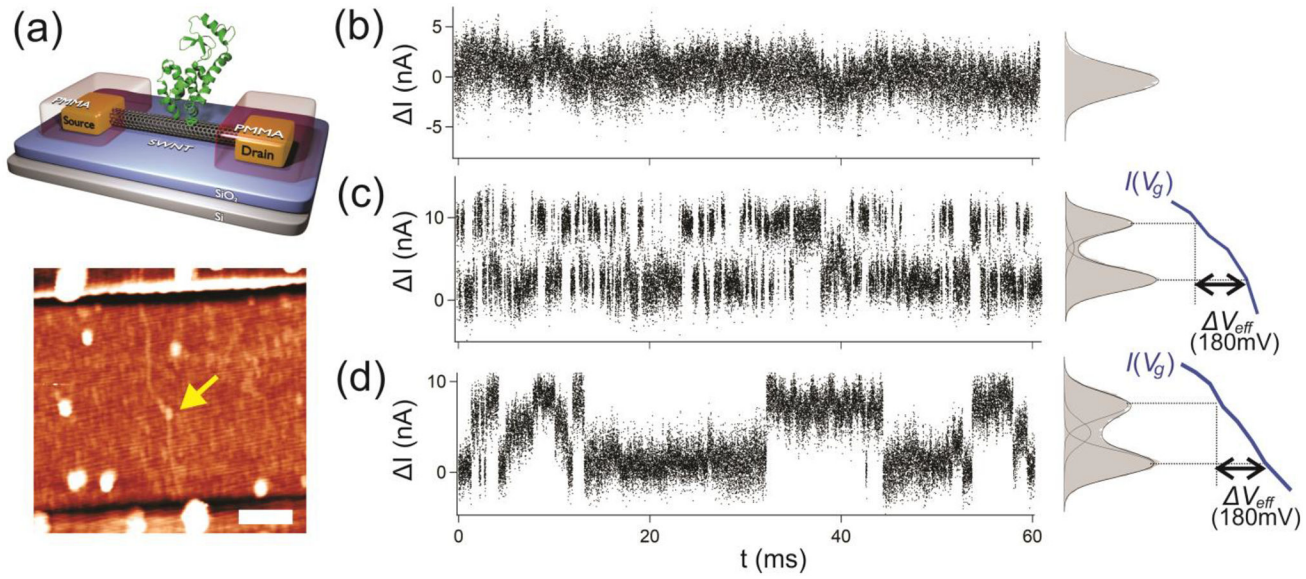

Figure 1.

Electronic recordings of lysozyme conformational dynamics. (a) A schematic diagram of the lysozyme nanocircuit (top) and an atomic force microscopy topography of the device showing a single lysozyme attached on the sidewall of SWNT (bottom, yellow arrow). The scale bar is 500 nm. (b) A small subset of $I(t)$ measured in the phosphate buffer and a histogram with Gaussian fit to a longer, 20-second segment. (c) Nonproductive motions of lysozyme with peptidoglycan substrate exhibited rapid two-level $I(t)$ fluctuations corresponding to lysozyme's open and closed conformations. The device $I(V_g)$ curve (right) determines the level spacing ΔV_{eff} that is a device-independent measure of the extent of conformational motion. (d) Catalytic motions of lysozyme with peptidoglycan substrate exhibited slower $I(t)$ fluctuations in which intermediate states are more clearly seen in both the signal and its histogram.

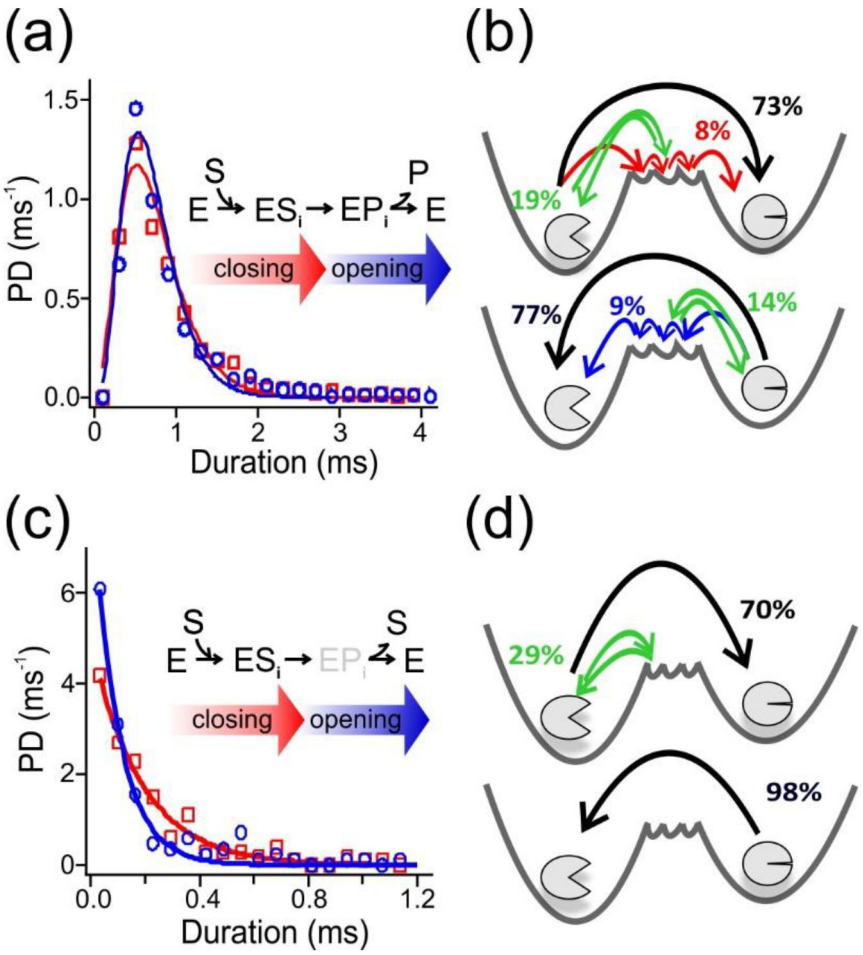

Figure 2.

Probability density (PD) of intermediate conformations with peptidoglycan substrate. (a) Pause durations during opening (blue circles) and closing (red squares) accumulated during slow, catalytic processing of the substrate. Solid curves display fits to the *N*-consecutive Poisson distribution (Eq. 1). The inset shows a schematic of the Michaelis-Menten mechanism, where E, S, P, and i indicate enzyme, substrate, product, and ith intermediate states, respectively. (b) Schematic diagrams illustrating conformational transitions with probabilities during closing (top) and opening (bottom) motions during the slow, catalytic process. (c) PD of opening (blue circles) and closing (red squares) durations accumulated from fast, nonproductive process. (d) Schematic diagrams illustrating conformational transitions with probabilities during the fast, nonproductive process. Transition probabilities lower than 2% are not indicated.

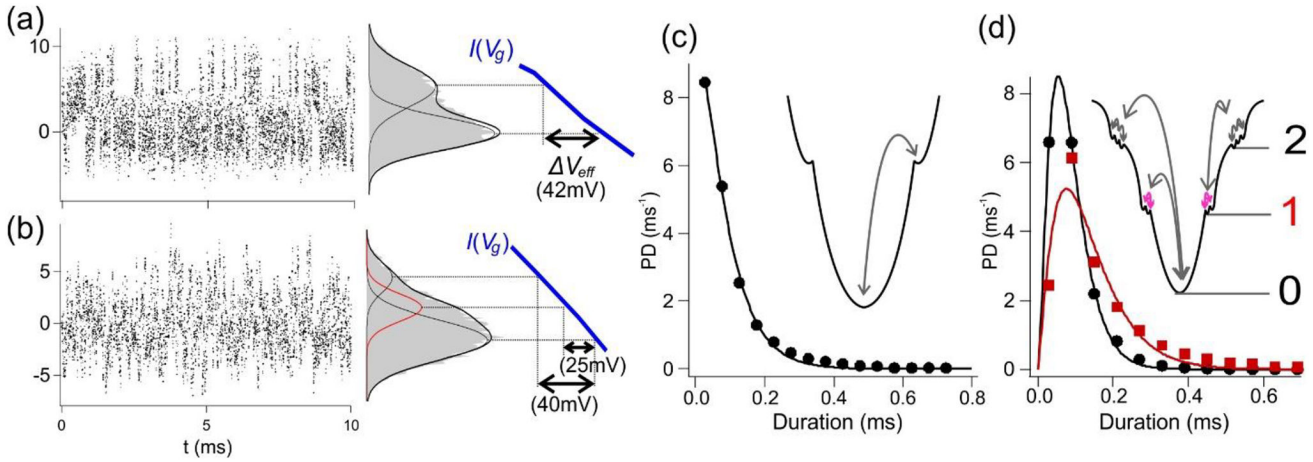

Figure 3.

Conformational dynamics of lysozyme with IPA and chitin. $I(t)$ measured in either (a) IPA or (b) chitin, with histograms, Gaussian peak fitting, and the ΔV_{eff} associated with each conformation. PDs for the durations of (c) the single excited conformation with IPA or (d) the two excited conformations with chitin, with solid lines for fits to the N-consecutive Poisson distribution (Eq. 1). Each inset depicts the potential well of lysozyme's open conformation and transient excursions to the excited conformations.

Table 1.

Conformational transition order and probability of lysozyme with chitin.

Transition	1st order		2nd order		3rd order		higher order	Total
	0-1-0	0-2-0	0-1-2-0	0-2-1-0	0-1-2-1-0	0-2-1-2-0		
Occurrence (%)	7660 (36.7)	7785 (37.2)	1499 (7.2)	1510 (7.2)	880 (4.2)	557 (2.7)	1003 (4.8)	20894 (100)